Solar Physics
DOI: 10.1007/•••••-•••-•••-••••-•

Correlation between Decay Rate and Amplitude of Solar Cycles as Revealed from Observations and Dynamo Theory

Gopal Hazra[1,3] · **Bidya Binay Karak**[2] · **Dipankar Banerjee**[3] · **Arnab Rai Choudhuri**[1]

© Springer ••••

Abstract Using different proxies of solar activity, we have studied the following features of solar cycle. (i) A linear correlation between the amplitude of cycle and its decay rate, (ii) a linear correlation between the amplitude of cycle n and the decay rate of cycle $(n-1)$ and (iii) an anti-correlation between the amplitude of cycle n and the period of cycle $(n-1)$. Features (ii) and (iii) are very useful because they provide precursors for future cycles. We have reproduced these features using a flux transport dynamo model with stochastic fluctuations in the Babcock-Leighton α effect and in the meridional circulation. Only when we introduce fluctuations in meridional circulation, we are able to reproduce different observed features of solar cycle. We discuss the possible reasons for these correlations.

Keywords: Solar cycle, observations; Solar cycle, models; Magnetic fields, models

1. Introduction

Solar cycles are asymmetric with respect to their maxima, the rise time being shorter than the decay time. While the cycle amplitude (peak value) and the duration have cycle-to-cycle variations, we find some correlations among different quantities connected with the solar cycle. Since 1935, it has been realized that the stronger cycles take less time to rise than the weaker ones (Waldmeier, 1935). This anti-correlation between rise times and peak values of the solar cycle is popularly known as the Waldmeier effect. Karak and Choudhuri (2011) have defined this aspect of the Waldmeier effect as WE1, whereas the correlation

[1] Department of Physics, Indian Institute of Science, Bangalore 560012, India
email: ghazra@physics.iisc.ernet.in
email: arnab@physics.iisc.ernet.in
[2] NORDITA KTH Royal Institute of Technology and Stockholm University, Roslagstullsbacken 23, SE-106 91 Stockholm, Sweden
email: bbkarak@nordita.org
[3] Indian Institute of Astrophysics, Bangalore 560034, India
email: dipu@iiap.res.in

arXiv:1410.8641v2 [astro-ph.SR] 7 May 2015

between the rise rates and the peak values is called WE2 (see also Cameron and Schüssler, 2008). Although WE2 is a more robust feature of the solar cycle, Karak and Choudhuri (2011) have shown that both WE1 and WE2 exist in many proxies of the solar cycle. WE2 provides a valuable precursor for predicting solar cycles because one can predict the strength of a cycle once it has just started (see Lantos, 2000; Kane, 2008).

The declining phase of the cycle also provides important clues for understanding long-term variations. We find that stronger cycles not only rise rapidly but also fall rapidly (shorter decay time). This results in a good correlation between the decay rate and amplitude of the same cycle. However, defining the decay rate differently, Cameron and Schüssler (2008) did not find a significant correlation between the decay rate and amplitude. Furthermore, we find a strong correlation between the decay rate of the current cycle and the amplitude of the next cycle, which was also found by Yoshida and Yamagishi (2010). The decay time, however, is found to have no correlation with the amplitude of the same cycle. Another important feature observed is that the amplitude of the cycle is inversely correlated with the period of the previous cycle (Hathaway, Wilson, and Reichmann, 2002; Solanki *et al.*, 2002; Ogurtsov and Lindholm, 2011). These two correlations again provide promising precursors to predict the strength of the future cycle (Solanki *et al.*, 2002; Watari, 2008).

Apart from showing these correlations from observational data, we also attempt to provide theoretical explanations for them. A dynamo mechanism operating in the solar convection zone is believed to be responsible for producing the solar cycle. It is generally accepted that the strong toroidal field (responsible for the formation of bipolar sunspots) is produced from the poloidal field by differential rotation in the solar convection zone (Parker, 1955a). This is the first part of solar dynamo theory. Due to magnetic buoyancy (Parker, 1955b) the flux tubes of toroidal field erupt out through the surface to form bipolar sunspot regions. These bipolar sunspots acquire tilts due to the action of the Coriolis force during their journey through the convection zone, giving rise to Joy's law (D'Silva and Choudhuri, 1993). To complete dynamo action, the toroidal field has to be converted back into the poloidal field. One possible mechanism for generating the poloidal field is the Babcock–Leighton (B-L) process (Babcock, 1961; Leighton, 1969), for which we now have strong observational support (Dasi-Espuig *et al.*, 2010; Kitchatinov and Olemskoy, 2011; Muñoz-Jaramillo *et al.*, 2013). In this process, the fluxes of tilted bipolar active regions spread on the solar surface through different processes (diffusion, meridional circulation, differential rotation) to produce the poloidal field. A model of the solar dynamo that includes a coherent meridional circulation and this B-L mechanism for the generation of the poloidal field is called the flux transport dynamo model. This model was proposed in the 1990s (Wang, Sheeley, and Nash, 1991; Durney, 1995; Choudhuri, Schussler, and Dikpati, 1995) and has been successful in reproducing many observed regular as well as irregular features of the solar cycle (Charbonneau and Dikpati, 2000; Küker, Rüdiger, and Schultz, 2001; Nandy and Choudhuri, 2002; Chatterjee, Nandy, and Choudhuri, 2004; Guerrero and Muñoz, 2004; Choudhuri and Karak, 2009; Hotta and Yokoyama, 2010; Karak

and Choudhuri, 2013). Recently Charbonneau (2010) , Choudhuri (2011) and Karak *et al.* (2014a) have reviewed this dynamo model.

An important ingredient in flux transport dynamo is the meridional circulation, which is not completely constrained either from observations or from theoretical studies. Until recently not much was known about the detailed structure of the meridional circulation in the convection zone (Zhao *et al.*, 2013; Schad, Timmer, and Roth, 2013). Therefore, most of the dynamo models use a single-cell meridional circulation in each hemisphere. However, very recently Hazra, Karak, and Choudhuri (2014) have shown that a complicated multi-cellular meridional circulation also retains many of the attractive features of the flux transport dynamo model if there is an equator-ward propagating meridional circulation near the bottom of the convection zone or if there is an equator-ward turbulent pumping (Guerrero and de Gouveia Dal Pino, 2008). While most of the calculations in this paper are done for a single-cell meridional circulation, we show that the results remain qualitatively similar for more complicated meridional circulations.

Since we want to do a theoretical study of the irregularities in the solar cycle, let us consider the sources of irregularities in the flux transport dynamo model that make different solar cycles unequal. At present we know two major sources: (i) variations in the poloidal field generation due to fluctuations in the B-L process (Choudhuri, Chatterjee, and Jiang, 2007; Goel and Choudhuri, 2009) and (ii) variations in the meridional circulation (Karak, 2010; Karak and Choudhuri, 2011). Direct observations of the polar field during last three cycles (Svalgaard, Cliver, and Kamide, 2005), as well as its proxies such as the polar faculae and the active network index available for about last 100 years (Muñoz-Jaramillo *et al.*, 2013; Priyal *et al.*, 2014), indicate large cycle-to-cycle variations of the polar field. The poloidal field generation mechanism mainly depends on the tilts of active regions, their magnetic fluxes and the meridional circulation, all of which have temporal variations. Particularly the scatter of tilt angles around the mean, caused by the effect of convective turbulence on rising flux tubes (Longcope and Choudhuri, 2002), has been studied by many authors (Wang and Sheeley, 1989; Dasi-Espuig *et al.*, 2010). Recently Jiang, Cameron, and Schüssler (2014) found that the tilt angle scatter led to a variation in the polar field by about 30% for cycle 17. In fact, even a single big sunspot group with large tilt angle and large area appearing near the equator can change the polar field significantly (Cameron *et al.*, 2013). On the other hand, for the meridional circulation, we have some surface measurements for about last 20 years, showing significant temporal variations (Chou and Dai, 2001; Hathaway and Rightmire 2010). Although our theoretical understanding of the meridional circulation is very limited, a few existing spherical global convection simulations do show significant variations in the meridional circulation (Passos, Charbonneau, and Beaudoin, 2012; Karak *et al.*, 2015). Introducing randomness in the poloidal field generation and in the meridional circulation, Karak and Choudhuri (2011) have been able to reproduce the Waldmeier effect in their high diffusivity dynamo model. When the meridional circulation becomes weaker, the cycle period and hence the rise time becomes longer. The longer cycle period allows the turbulent diffusion to act for a longer time, making the cycle amplitude weaker (Yeates,

Nandy, and Mackay, 2008; Karak, 2010) and leading to the Waldmeier effect. The variation of the meridional circulation is crucial in reproducing this effect.

The motivation of the present work is to explore how the decay rates of cycles are related to their amplitudes in a flux transport dynamo model, with the aim of explaining the observed correlations mentioned earlier. The presentation of the paper is following. In the next section, we summarize some of the features of solar cycle that are often considered as precursors of the solar cycle. In Section 3, we present a brief summary of our flux transport dynamo model and then in Sections 4 we introduce suitable stochastic fluctuations in the poloidal field and the meridional circulation, in order to reproduce various observed features of the solar cycle. Finally the last section summarizes our conclusions.

2. Observational Studies

We have used three different observational data sets: (i) Wolf sunspot number[1] (cycles 1–23), (ii) sunspot area[2] (cycles 12–23), and (iii) 10.7 cm radio flux[3] (available only for the last five cycles). These parameters are very good proxies of magnetic activity and are often used to study the solar cycle (Hathaway *et al.* 2002). To minimize the noise while keeping the underlying properties unchanged, we smooth these monthly data using a Gaussian filter having a full-width at half maximum (FWHM) of 1 year. We also average the data with FWHM of 2 years to check how the results change with the filtering.

2.1. Correlation between the Decay Rate and the Cycle Amplitude

We have calculated the decay rate at three different phases of the descending phase of the cycle, namely, early phase, late phase and entire phase. For the early phase, the decay rate is taken as the slope between two points with a separation of 1 year with the first point one year after the cycle peak, whereas for the late phase the second point is taken 1 year before the cycle minimum. Here we exclude one year after the maximum when computing decay rate for the early phase because sometimes the cycle peaks are not so prominent. While computing the decay rate for the late phase we also exclude 1 year before the minimum just to avoid the effect of overlapping between two cycles during solar minimum. Finally, the decay rate of the entire decay part (*i.e*, entire phase) is taken as the average of the individual decay rates computed at four different locations with a separation of one year starting from early phase to the late phase. In Figure 1 (a), (b) and (c), we show the correlations of the cycle amplitudes with the decay rates of the entire phase computed from sunspot number, sunspot area and 10.7 cm radio flux data, respectively.

We would like to point out that Cameron and Schüssler (2008) have computed the decay rate from the intervals of two fixed values of solar activity and they

[1]http://solarscience.msfc.nasa.gov/greenwch/spot_num.txt

[2]http://solarscience.msfc.nasa.gov/greenwch/sunspot_area.txt

[3]http://www.ngdc.noaa.gov/stp/solar/flux.html

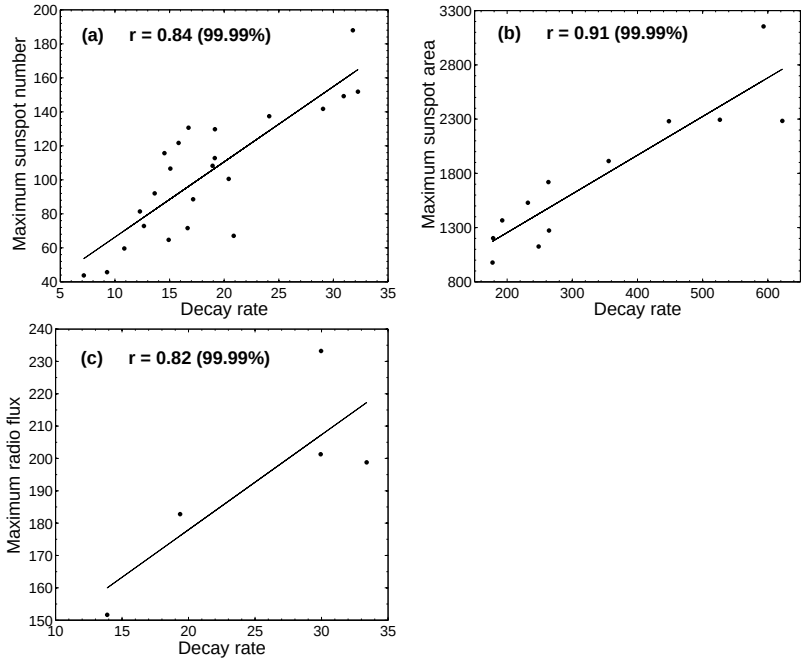

Figure 1. Scatter plots of the decay rate and the amplitude of the same cycle computed from (a) sunspot number, (b) sunspot area, and (c) 10.7 cm radio flux data. In all these cases the original monthly data are smoothed using a Gaussian filter with FWHM of 2 years.The straight line in each plot is best linear fit of data. The correlation coefficients (r) and the significance levels are also given in each plot.

did not get significant correlation between the decay rate and the amplitude (see right column, Figure 2 of their paper). The reason of not finding significant correlation is that they have calculated the decay rate in the late phase of the cycle, *i.e.* near the tail of the cycle where the rate of decay is really very small. We find that their values are comparable with our decay rates computed in the late phase. In 4th and 5th columns of Table 1 we have listed our values and the values computed following Cameron and Schüssler (2008) method (hereafter referred as CS08). It is interesting to note that even for the radio flux data for which we have only five data points, we get strong correlation; see Table 1 for details. Therefore we can see that if we determine the decay rates from the entire phase of the solar cycle or the early phase, we find strong correlation with the amplitude. Thus, to determine the decay rate from descending part of the solar cycle, we need to consider the entire decay phase of the cycle, which provides a better estimate than CS08.

2.2. Correlation between the Decay Rate and the Next Cycle Amplitude

Next we find that there is a significant correlation between the amplitude of cycle and the decay rate of the previous cycle. Again we find this correlation for all the data sets considered here (see Table 1). However in Figure 2(a) we

Table 1. Correlation coefficients between different quantities of the solar cycle.

Data set	FWHM	Correlation coefficients of the decay rate with the amplitude of						Correlation between the amplitude and the previous cycle period
		Same cycle				Next cycle		
		Entire phase	Late decay phase		Early Phase	Entire phase	Late phase	
			Our value	CS08's value				
Sunspot number	1 yr	0.79	0.21	0.22	0.67	0.55	0.61	-0.64
	2 yr	0.86	0.45	–	0.86	0.65	0.83	-0.67
Sunspot area	1 yr	0.84	0.20	0.11	0.69	0.14	0.37	-0.49
	2 yr	0.91	0.53	–	0.92	0.39	0.66	-0.60
Radio flux	1 yr	0.86	-0.11	0.14	0.93	-0.42	0.64	0.11
	2 yr	0.82	0.24	–	0.95	-0.43	0.46	0.09

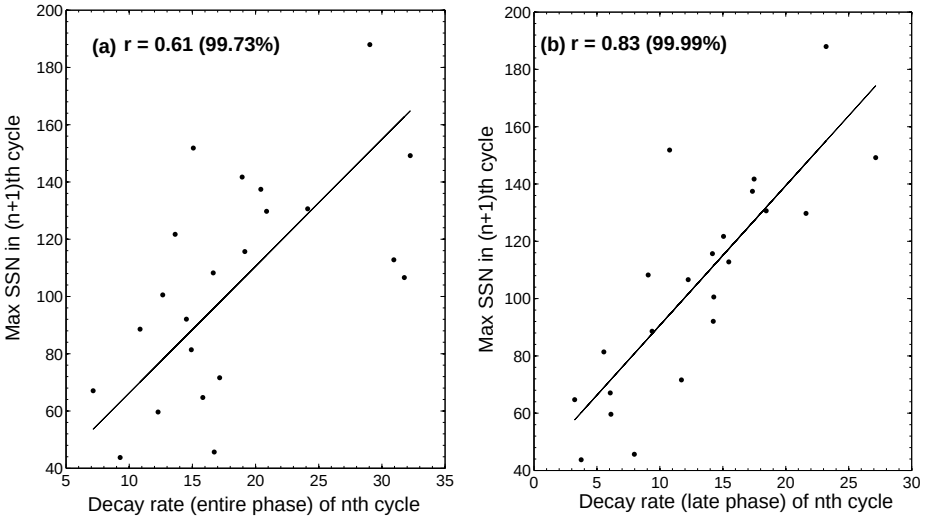

Figure 2. Scatter plots showing the correlation of the amplitude vs. the decay rate of the previous cycle computed from sunspot number data (smoothed with FWHM of 2 year). In (a) the decay rate is computed from the entire decay phase, whereas in (b) it is at late decay phase.

show this correlation only for sunspot number. Note that here the decay rates have been calculated from the entire decay phase as discussed in Section 2.1. This correlation suggests that the decay rate of a cycle carries some information of the strength of the next cycle. It is interesting to note that when we look at this correlation with the decay rate computed in the late phase, the correlations become even stronger; see Figure 2(b). In 7th and 8th column of Table 2, we show both correlations for all three data sets. These results suggest that particularly

the late phase of the cycle carries more information of the forthcoming cycle. This correlation of decay rate with the amplitude of succeeding cycle is already reported in Yoshida and Yamagishi (2010). They have shown this correlation for only sunspot number data and their methodology for calculation of decay rate (rate of decrease in sunspot number over some time) is somewhat different from our methodology. They have studied decay rate in six different cases (see their Figures 1(a)-(f)). They have obtained the decay rate from the decrease of sunspot number (SSN) over the period of 1, 2, 3, 4, 5 and 6 years before the minima of the cycle in the six different cases of study respectively. Since solar cycles sometimes have overlapping regions during minima and it is difficult to ascertain the actual minima, there are some uncertainties in the methodology of Yoshida and Yamagishi (2010). The correlation coefficient ($r = 0.70$) obtained in the second case of their study (see their Figure 1(b)) should be the same with what we obtained during late phase correlation ($r = 0.83$). Since they have not considered the overlapping region between the minima and used monthly smoothed SSN, the value of the correlation coefficient is slightly different.

Cameron and Schüssler (2007) (also see Brown, 1976) have observed similar feature that the activity level during the solar minimum is an indicator for the strength of the next solar cycle and argued that this is caused by overlap between two cycles during solar minimum.

In all our theoretical calculations (subsequent section), while studying the correlation between the amplitude and the decay rate of the same cycle, we shall consider the decay rate of the entire phase, but for the correlation with the next cycle we shall consider only the late-phase decay rate.

Since the decay rate of the cycle n is correlated both with the amplitude of cycle n (Figure 1) and the amplitude of cycle $n + 1$ (Figure 2), one question that naturally arises is whether the amplitude of cycle n and the amplitude of cycle $n + 1$ are themselves correlated. We show a correlation plot between these amplitudes in Figure 3, demonstrating that there is not a significant correlation. The challenge before a theoretical model is, therefore, to explain how the decay rate of cycle n is correlated both with the amplitude of cycle n and the amplitude of cycle $n+1$, while these amplitudes themselves do not have a strong correlation.

2.3. Correlation between the Cycle Period and the Next Cycle Amplitude

Finally, we also find that the shorter cycles are followed by stronger cycles and vice versa. This produces an anti-correlation between the amplitude of a cycle and the period of the previous cycle (Hathaway, Wilson, and Reichmann, 2002; Solanki *et al.*, 2002; Ogurtsov and Lindholm, 2011). Figure 4 shows this correlation from sunspot number data (smoothed using a Gaussian filter with FWHM of 2 years). The correlation coefficients from other data are listed in Table 1. For all data we have taken the period of the cycle just as the time difference between two successive minima.

3. Theoretical Framework of the Dynamo Model

We carry out our theoretical studies using the flux transport dynamo model originally presented by Chatterjee, Nandy, and Choudhuri (2004). In this model,

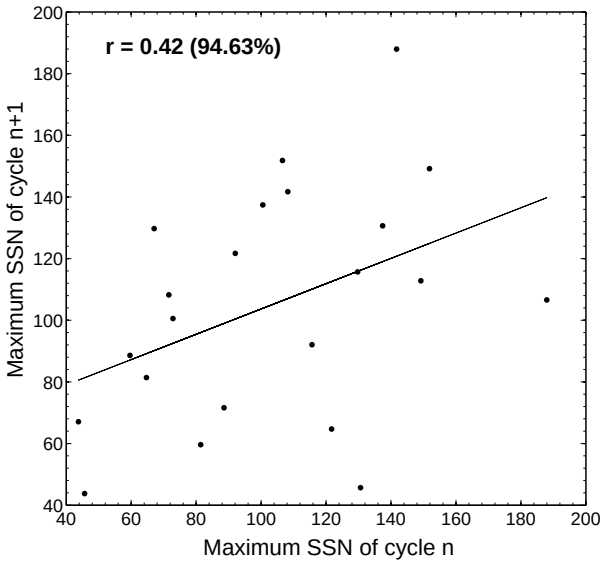

Figure 3. Scatter plot of nth cycle amplitude and the amplitude of the next $n+1$ cycle from sunspot number data (smoothed with FWHM of 2 years).

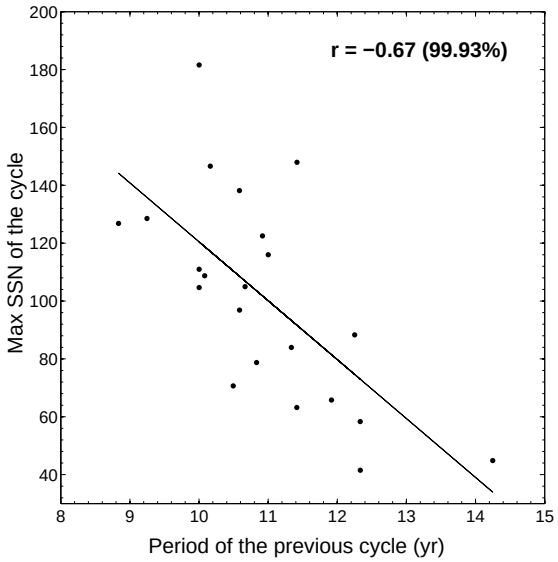

Figure 4. Scatter plot showing the anti-correlation between the cycle amplitude and the period of the previous cycle from sunspot number data (smoothed with FWHM of 2 years).

the evolution of the axisymmetric two-dimensional magnetic field is governed by following two equations:

$$\frac{\partial A}{\partial t} + \frac{1}{s}(\mathbf{v}.\nabla)(sA) = \eta_{\rm p}\left(\nabla^2 - \frac{1}{s^2}\right)A + S_{\rm BL}(r,\theta;B), \tag{1}$$

$$\frac{\partial B}{\partial t} + \frac{1}{r}\left[\frac{\partial}{\partial r}(rv_rB) + \frac{\partial}{\partial \theta}(v_\theta B)\right] = \eta_{\rm t}\left(\nabla^2 - \frac{1}{s^2}\right)B + s(\mathbf{B}_{\rm p}.\nabla)\Omega + \frac{1}{r}\frac{d\eta_{\rm t}}{dr}\frac{\partial B}{\partial r}, \tag{2}$$

where $s = r\sin\theta$, $B(r,\theta)$ is the toroidal component of the magnetic field , $A(r,\theta)$ is the vector potential of the poloidal field, $\mathbf{v} = v_r\hat{\mathbf{r}} + v_\theta\hat{\theta}$ is the velocity of the meridional flow, Ω is the internal angular velocity of the Sun and $\eta_{\rm t}$, $\eta_{\rm p}$ are the turbulent diffusivities of the toroidal and the poloidal fields. Since the detailed discussion of the parameters and boundary conditions are given in Chatterjee, Nandy, and Choudhuri (2004) and Karak and Choudhuri (2011), here we do not discuss them again. We only make a few remarks about magnetic buoyancy and about the term $S_{\rm BL}(r,\theta;B)$ appearing in Equation (1), which captures the longitude averaged B-L mechanism.

Let us discuss how the magnetic buoyancy is treated in this model. When the toroidal field above the tachocline ($r = 0.71R_\odot$) at any latitude exceeds a certain value, a fraction of it is reduced there and the equivalent amount of this field is added on the solar surface. Then this local toroidal field near the surface is multiplied by a factor α to give the poloidal field. The source term in Equation (1), therefore, is

$$S_{\rm BL}(r,\theta;B) = \alpha B(r,\theta,t), \tag{3}$$

where

$$\alpha = \frac{\alpha_0}{4}\cos\theta\left[1 + {\rm erf}\left(\frac{r - 0.95R_\odot}{0.03R_\odot}\right)\right]\left[1 - {\rm erf}\left(\frac{r - R_\odot}{0.03R_\odot}\right)\right], \tag{4}$$

with $\alpha_0 = 30$ m s^{-1}. Now our job is to use this model to study the observed features of solar cycle reported in previous sections. To study any irregular feature of the solar cycle, we have to make the cycles unequal by introducing randomness in this regular dynamo model, as we discuss in the following sections.

In most of our calculations, we have followed Chatterjee, Nandy, and Choudhuri (2004) in assuming the meridional circulation to consist of one cell. Of late, this assumption has been questioned, although the exact nature of the meridional circulation in the deeper layers of the convection zone is still not known. We have shown in Section 4.4 that we can retain the attractive features of our results with more complicated meridional circulation (Hazra, Karak, and Choudhuri 2014). We have also included the near-surface shear layer in the calculations presented in Section 4.4.

4. Results of Theoretical Modeling

4.1. Fluctuations in the Poloidal Field Generation

We have discussed in the Introduction that the Sun does not produce equal amount of poloidal field at the end of every cycle and that the generation of the poloidal field involves randomness. Therefore, similar to adding stochastic fluctuations in the traditional mean-field alpha (Choudhuri, 1992), adding stochastic fluctuations in the B-L α has become a standard practice in the flux transport dynamo community (Charbonneau and Dikpati, 2000; Jiang, Chatterjee, and Choudhuri, 2007; Karak and Nandy, 2012). In the present work, first we introduce stochastic noise in the B-L α in the following way:

$$\alpha_0 \rightarrow \alpha_0 + \sigma(t,\tau)\alpha_0', \tag{5}$$

where τ is the coherence time during which the fluctuating component remains constant and σ is a uniformly distributed random number in the interval [-1, 1]. Considering the typical decay time of the active regions by surface flux transport process, we fix the coherence time within 0.5 – 2 months. To see a noticeable effect, we add 75% fluctuations in α (*i.e.*, $\alpha_0'/\alpha_0 = 0.75$) with coherence time of 1 month. From this stochastically forced model we have to calculate a measure of the theoretical sunspot number. We consider the magnetic energy density (B^2) of toroidal field at latitude 15° at the base of the convection zone ($r = 0.7R_\odot$) as a proxy of sunspot number (this was done by Charbonneau and Dikpati, 2000). Note that absolute value of the theoretical sunspot number does not have any physical meaning. Therefore, we scale it by an appropriate factor to match it with the observed sunspot number. From the time series of theoretical sunspot number, we calculate the cycle periods and decay rates in the same way as we have done for the observational data.

In Figure 5(a) we show the correlation between the decay rates and the amplitudes of the same cycles. We see a positive correlation as in the observed data presented in Figure 1. It is easy to understand the reason behind getting this positive correlation. Since we have kept meridional circulation fixed, the periods of the solar cycle do not vary much but the cycle strengths do vary due to the fluctuations in the poloidal field generation. Therefore, when the amplitude of a cycle increases while its period remains approximately fixed, the cycle has to decay rapidly. Hence we find that the stronger cycles decay faster than the weaker cycles, producing the positive correlation seen in Figure 5(a). However, we see in Figure 5(b) that there is not much correlation between the decay rate of the cycle n and the amplitude of the next cycle $n + 1$ and we are unable to explain the observed correlation seen in Figure 2. Note that for Figure 5(a) the decay rates are calculated from the entire decaying part of the cycle which is more appropriate definition of the decay rate as we argued in Section 2, whereas for Figure 5(b) it is computed at the late decay phase because observationally we find strong correlation when decay rate is computed in late decay phase only. Finally we see in Figure 5(c) that in this study the observed anti-correlation

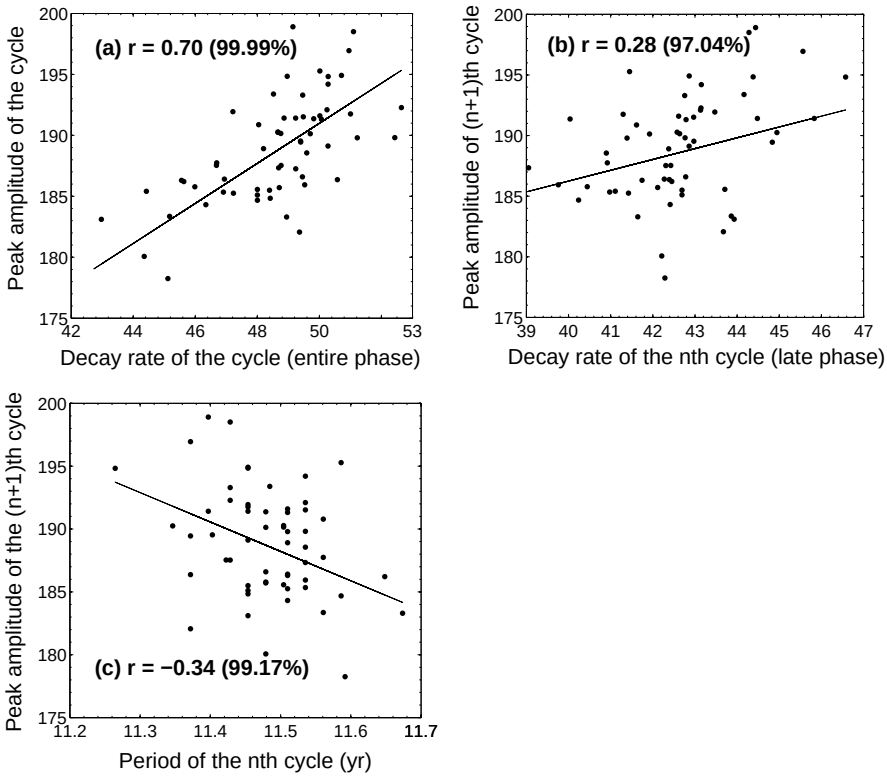
(a) r = 0.70 (99.99%)
Peak amplitude of the cycle
Decay rate of the cycle (entire phase)
(b) r = 0.28 (97.04%)
Peak amplitude of (n+1)th cycle
Decay rate of the nth cycle (late phase)
(c) r = −0.34 (99.17%)
Peak amplitude of the (n+1)th cycle
Period of the nth cycle (yr)

Figure 5. Results from stochastically forced dynamo model with B-L α fluctuations: Scatter plots showing the correlations between (a) the decay rate and the amplitude of cycle n, (b) the decay rate of cycle n and the amplitude of cycle $n+1$, (c) the period of cycle n and the amplitude of cycle $n+1$.

between the period of cycle n and the amplitude of cycle $n+1$ (shown in Figure 4) is also not reproduced. Note that the period does not vary too much when the meridional circulation is kept constant.

To sum up, when we introduce fluctuations in the poloidal field generation mechanism, we can explain the observed correlation between the decay rate and the amplitude of the cycle shown in Figure 1, but we cannot explain the other observed correlations presented in Figures 2 and 4.

4.2. Fluctuations in the Meridional Circulation

Next we introduce the other important source of fluctuations in the flux transport dynamo model, namely, variations of the meridional circulation. Although we have some observational results of the meridional circulation variations near the solar surface for the last 15 – 20 years, we do not have long data to conclude the nature of long-term variations (Chou and Dai, 2001; Hathaway and

Rightmire, 2010). However, there are indirect evidences for the variation of the meridional circulation over a long time (Lopes and Passos, 2009; Karak, 2010; Passos and Lopes, 2012). Particularly, Karak and Choudhuri (2011) have used the durations of the past cycles to argue that the meridional circulation has long-term variations with the coherence time of probably 20 – 45 years. There can also be short-term variations in the meridional circulation whose time scale may be related to the convective turnover time of the solar convection zone. Such variations with the time scale from a few months to a year are also observed in global magnetohydrodynamic simulations (Karak *et al.*, 2014b). In this work, we vary the amplitude of the meridional circulation in the same way as we have done for the α term but with a different coherence time. We show the results of simulations with 30% fluctuations in the meridional circulation with coherence time of 30 years. We shall discuss later that various observed correlations can be explained only if the coherence time is assumed to be not much less than the cycle period. While fluctuations of shorter duration (along with spatial variations) are likely to be present in the meridional circulation, we believe that they do not play any role in producing the correlations we are studying. With 30% level of fluctuations with a coherence time of 30 years, we get variations of the amplitude and of the period in our theoretical model comparable to the observational data. As in Section 4.1, we take the time series (B^2) at latitude 15° at the base of the convection zone as our proxy of sunspot activity and calculate the required correlations from it. The relevant correlation plots are shown in Figure 6. We see in Figure 6(a) that now the correlation between the decay rates and the cycle amplitudes has improved. Importantly, the other correlations are also correctly reproduced in Figures 6(b) and 6(c) and can be compared with the observational plots Figure 2(b) and Figure 4. These correlations did not appear at all when the fluctuations in poloidal field generation was introduced (*cf.* Figures 5(b) and 5(c)). To show how the correlations change on changing the correlation time or the level of fluctuations, we tabulate the values of correlations coefficients under different situations in Table 2. Each correlation coefficient is calculated from a run of 50 cycles. It should be kept in mind that there is some statistical noise in the values of correlation coefficients. If the correlation coefficient for exactly the same set of parameters is calculated from different independent runs, the values for different runs will be a little bit different. Keeping this in mind, we note that there is no clear trend of the correlation coefficients increasing or decreasing with increasing levels of fluctuations (other things being the same). However, all the correlation coefficients tend to decrease on decreasing the coherence time.

It is not difficult to understand how the correlation in Figure 6(a) arises. For a stronger cycle, the sunspot number has to decrease by a larger amount during the decay phase, making the decay rate faster. However, to understand the physical reason behind the other two correlations seen in Figures 6(b) and 6(c), more subtle arguments are needed. Karak and Choudhuri (2011) extended the arguments of Yeates, Nandy, and Mackay (2008) and pointed out that a weaker meridional circulation, which makes the cycles longer, will have two effects. Firstly, the differential rotation has more time to generate more toroidal field and tends to make the cycles stronger. Secondly, the turbulent diffusivity gets more time to act on the fields and tends to make the cycles weaker. When

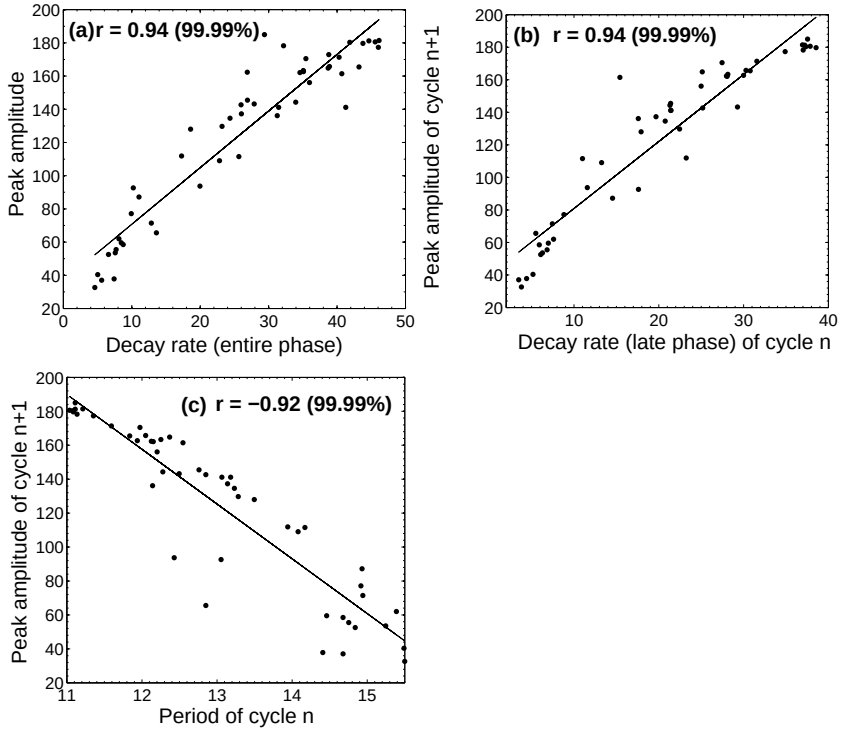
(a)r = 0.94 (99.99%)
Peak amplitude
Decay rate (entire phase)
(b) r = 0.94 (99.99%)
Peak amplitude of cycle n+1
Decay rate (late phase) of cycle n
(c) r = −0.92 (99.99%)
Peak amplitude of cycle n+1
Period of cycle n

Figure 6. Same as Figure 5 but with meridional circulation fluctuations.

the diffusivity is high (as in our model), the second effect dominates over the first and the longer cycles are weaker (the opposite is true for dynamo models with low diffusivity). Karak and Choudhuri (2011) showed that this led to an explanation of the Waldmeier effect for dynamo models with high diffusivity. We now point out that this tendency (longer cycles tending to be weaker) is also crucial in our understanding of the correlations seen in Figures 6(b) and 6(c).

If the meridional circulation keeps fluctuating with a coherence time of 30 years, it would happen very often that the meridional circulation would have a certain value during a cycle (say cycle n) and the early rising phase of the next cycle (say cycle $n + 1$). This is less likely to happen when the coherence time is reduced. Suppose the meridional circulation is weaker during cycle n and the rising phase of cycle $n + 1$. Then cycle n will tend to be longer and to have a weaker decay rate. The following cycle $n + 1$ will have a tendency of being weaker. This will produce the correlations seen in Figures 6(b) and 6(c). On decreasing the coherence time, it will happen less often that the meridional circulation will be the same during cycle n and the rising phase of the next cycle $n + 1$. Hence the correlations degrade on decreasing the coherence time of the meridional circulation.

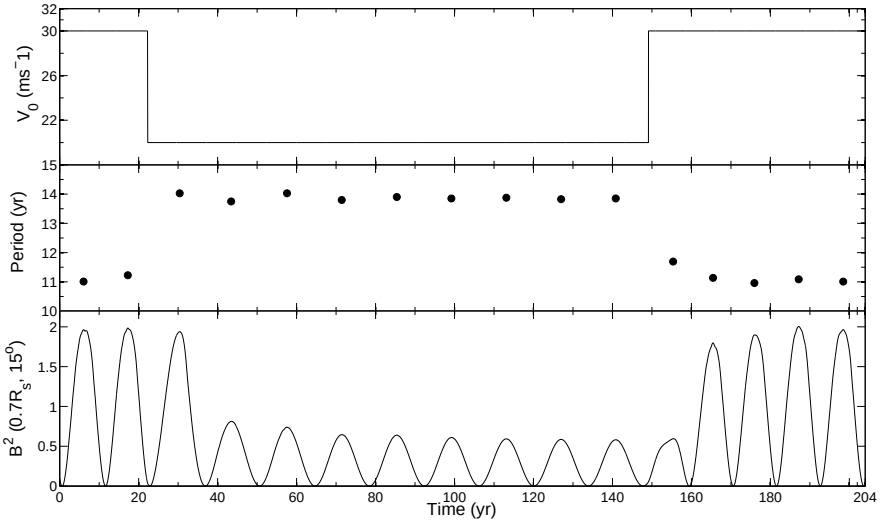

Figure 7. Plots showing how the variation of meridional circulation, measured by v_0, with time (upper panel) changes the period of the cycle (middle panel) and strength of the magnetic field (shown by B^2 in the lower panel).

We have realized that there is also a memory effect, which enhances the correlations explained in the previous paragraph. To illustrate this memory effect, we make a run of our dynamo code in which the meridional circulation is decreased suddenly during a sunspot minimum and then brought back to its original value during another sunspot minimum a few cycles later. The meridional circulation and the resulting sunspot activity are plotted in Figure 7. The periods of successive cycles are also indicated in the middle panel of Figure 7. On changing the meridional circulation, it is found that the periods of cycles begin changing almost immediately. However, there seems to be a memory effect as far as the amplitudes of the cycles are concerned. Even after the meridional circulation changes, the amplitude of the next cycle is very similar to the amplitude corresponding to the earlier value of the meridional circulation. This memory effect will certainly enhance the correlations we are discussing. Suppose the meridional circulation is weaker during the cycle n, making its period longer and decay rate weaker. Even if the meridional circulation becomes stronger by the rising phase of the next cycle $n+1$, the memory effect will ensure the amplitude of the cycle $n+1$ will still be weak, thereby producing the correlation.

At this point, we would like to mention a misconception behind the correlation between cycle n period and cycle $n+1$ amplitude. It may be thought that the overlap between two cycles during solar minimum is the cause of this correlation. If the next cycle is stronger, then it starts early and the overlap with the present cycle is more. This makes the present cycle shorter. However we believe that this is not the source of this correlation because if this is so, then we would have seen this correlation in Figure 5(c) also, where cycle strengths were varied by fluctuations in the poloidal field generation. So the overlap is not the reason

behind this correlation and we only get this in high diffusivity dynamo model with fluctuating meridional circulation.

Table 2. Correlation coefficients at different levels of fluctuations and coherence time of meridional circulation.

Coherence time (year)	Fluctuations (%)	Correlation of decay rate with cycle amplitude of		Correlation of previous cycle period with amplitude
		Same cycle (Entire phase)	Next cycle (Late phase)	
30	10	0.92	0.92	-0.97
	20	0.86	0.92	-0.95
	30	0.87	0.89	-0.96
	40	0.92	0.96	-0.73
	50	0.87	0.91	-0.94
20	10	0.79	0.85	-0.95
	20	0.86	0.86	-0.98
	30	0.93	0.96	-0.97
	40	0.90	0.87	-0.88
	50	0.89	0.90	-0.97
11	10	0.78	0.74	-0.90
	20	0.88	0.77	-0.97
	30	0.90	0.85	-0.92
	40	0.82	0.74	-0.89
	50	0.82	0.84	-0.83
5.5	10	0.70	0.63	-0.87
	20	0.83	0.74	-0.86
	30	0.81	0.79	-0.84
	40	0.81	0.57	-0.85
	50	0.80	0.81	-0.78
1	10	0.57	0.48	-0.78
	20	0.58	0.59	-0.64
	30	0.61	0.67	-0.80
	40	0.73	0.25	-0.65
	50	0.69	0.38	-0.72
	75	0.64	0.39	-0.58
	100	0.65	0.73	-0.76
0.5	10	0.42	0.62	-0.80
	20	0.56	0.69	-0.78
	30	0.68	0.47	-0.74
	40	0.62	0.56	-0.67
	50	0.61	0.56	-0.79
	75	0.64	0.50	-0.81
	100	0.64	0.60	-0.87

4.3. Fluctuations in the Poloidal Field Generation and the Meridional Circulation

Finally we add fluctuations in both the poloidal field generation process and the meridional circulation of the regular model, which is the realistic scenario. We add the same amount of fluctuations in poloidal field generation and in meridional circulation that we had added earlier in the individual cases (*i.e.*, 75% fluctuations in the poloidal field generation with a coherence time of 1 month and 30% fluctuations in the meridional circulation with a coherence time of 30 years). The results are shown in Figures 8. In this figure, we see that the scatters in the correlation plots are very close to what we find in actual observations. It is perhaps not a big surprise that all the correlations are reproduced correctly, because they were already reproduced on introducing fluctuations in meridional circulation alone.

A correct theoretical model also should explain the lack of correlation seen in Figure 3 between peaks of two successive cycles. Figure 9(a) shows the correlation between the amplitude of cycle n and the amplitude of cycle $n+1$ for the same level of fluctuations which were used to generate Figure 8, whereas Figure 9(b) gives the same correlation when the fluctuation is B-L α is raised to 100% from 75%. It is seen that the correlations between these amplitudes is weak and becomes weaker still on increasing the fluctuation in the B-L α. A physical interpretation is not difficult to give. A coherence time of 30 years in meridional circulation implies that very often the meridional circulation will be the same during two successive cycles, trying to produce a correlation between the cycles. On the other hand, a fluctuation in the B-L α will definitely try to reduce the correlation. Certainly this fluctuation would try to reduce the correlations seen in Figure 8 as well. However, for our choice of parameters, we are able to theoretically reproduce the three observed correlations as seen in Figure 8, whereas the correlation between successive cycles is much weaker in conformity with observations. We may mention that we also get an anti-correlation between the amplitude of a cycle and its duration. Our theoretical correlation coefficient ($r = -0.65$) is somewhat stronger than what Charbonneau and Dikpati (2000) obtained from the observational data ($r = -0.37$).

4.4. Robustness of the Results on Changing the Meridional Circulation and Differential Rotation Profiles

So far, our earlier computations are performed using a single-cell meridional circulation in each hemisphere. However, recent observations, helioseismic inversions and convection simulations suggest the possibility that the meridional circulation may have a complicated multi-cellular structure rather than being single-cellular (*e.g.*, Zhao *et al.,* 2013; Karak *et al.,* 2015). In Hazra, Karak, and Choudhuri (2014), we have shown that the flux transport dynamo model can reproduce most of basic features of solar cycle using multi-structured meridional circulation as long as there is an equator-ward flow near the bottom of the convection zone. Therefore we are curious to know whether the correlations studied in this paper are also reproduced with multi-structured circulation. To answer

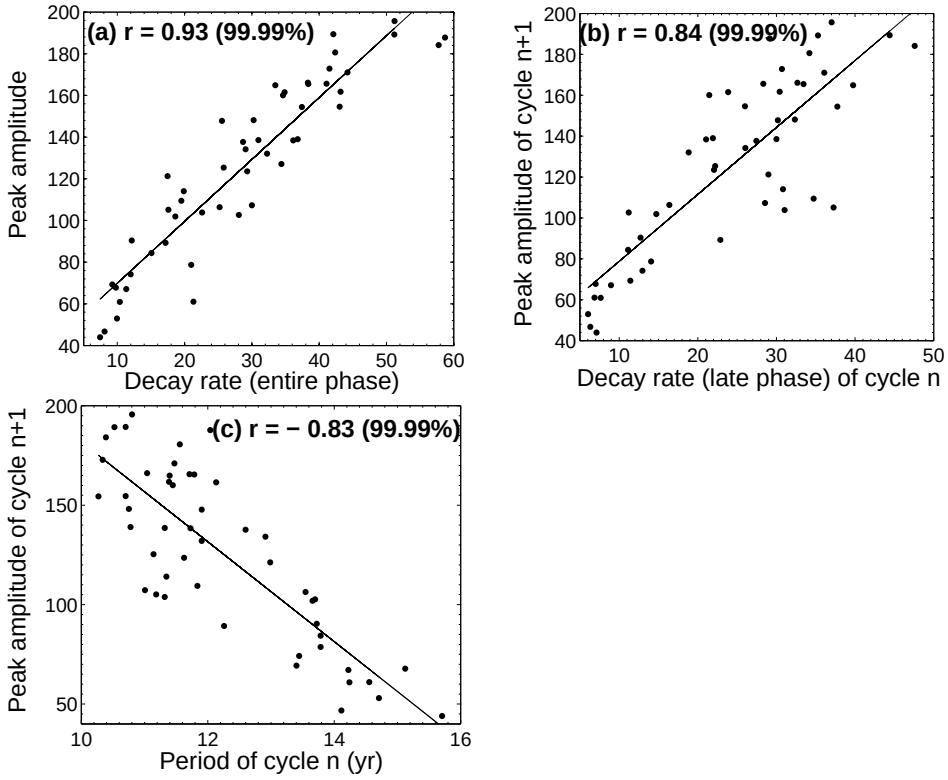
(a) r = 0.93 (99.99%)
Peak amplitude
Decay rate (entire phase)
(b) r = 0.84 (99.99%)
Peak amplitude of cycle n+1
Decay rate (late phase) of cycle n
(c) r = − 0.83 (99.99%)
Peak amplitude of cycle n+1
Period of cycle n (yr)

Figure 8. Same as Figure 5 but with both B-L α and meridional circulation fluctuations.

this question, we perform a simulation with three radially stacked circulation cells, exactly the same as used in Section 3 of Hazra, Karak, and Choudhuri (2014). For the differential rotation in all our previous works, we have used a simplified profile of the observed differential rotation that does not capture the near-surface shear layer (see *e.g.* Figure 1 of Chatterjee *et al.,* 2004). Although it is expected that the near-surface shear layer does not produce significant effect on global large-scale fields in the flux transport dynamo (Dikpati *et al.*, 2002), just for the sake of completeness we use a somewhat improved profile of differential rotation captured by the following analytical formula

$$\Omega(r,\theta) = \sum_{j=0}^{2} \cos\left(2j\left(\frac{\pi}{2}-\theta\right)\right) \sum_{i=0}^{4} c_{ij}(r/R_\odot)^i. \tag{6}$$

For the coefficients c_{ij} see Table 1 of Belvedere, Kuzanyan, and Sokoloff (2000), (see also their Figure 1 for the comparison with observed profile).

With these new profiles of the meridional circulation and the differential rotation, we perform a dynamo simulation by adding the same amount of stochastic fluctuations in B-L α and in meridional circulation as done in the previous sec-

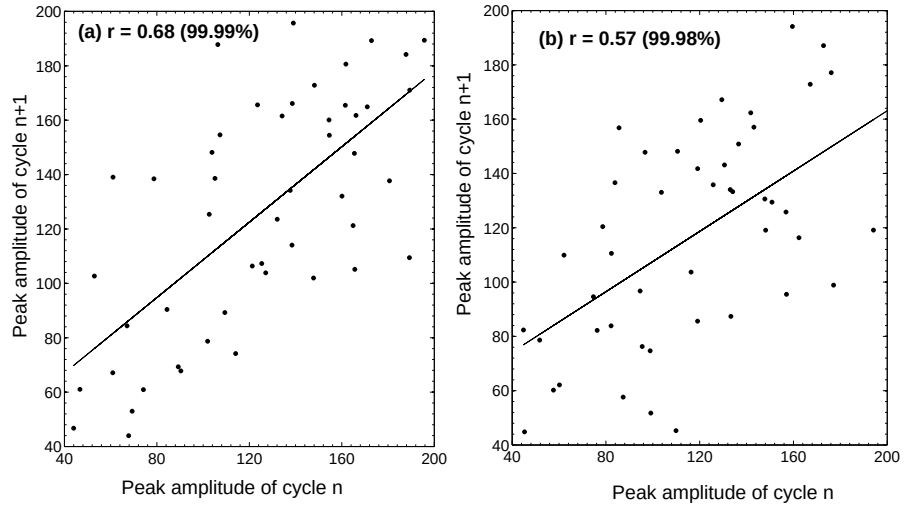

Figure 9. (a) Scatter plot of the amplitude of cycle n with the amplitude of cycle $n+1$ with 75% fluctuation in B-L α. (b) Same as (a) but with 100% fluctuation in B-L α.

tion. In the results presented earlier, magnetic buoyancy was treated by moving a part of the toroidal magnetic field to the surface whenever it became larger than a critical value. However, as pointed out in Hazra, Karak, and Choudhuri (2014) and Karak, Kitchatinov, and Choudhuri (2014), this way of treating magnetic buoyancy is not very robust under a large change in parameters and model ingredients. Therefore, for the computations of this section we use the 'non-local' magnetic buoyancy as used in Charbonneau and Dikpati (2000), and in many other works.

Final results from this computation are shown in Figure 10. We observe that even with the *unconventional* meridional flow profile (three radial cells) and addition of near-surface shear layer, the correlations do not disappear. Although the correlations in Figures 10(b) and 10(c) become a little weaker compared to what we have found for the usual single-cell circulation (Figure 8), they show the correct general features as found in observations. The values of the correlations might be improved a little bit by tuning the amount of imposed fluctuations; we do not want to do that here, rather we have used same amount of fluctuations as we used in earlier sections.

We make a few remarks about the two ways of treating magnetic buoyancy. The behaviour of the dynamo can become substantially different on treating magnetic buoyancy in these two different ways (Choudhuri, Nandy, and Chatterjee, 2005). Since some magnetic field is removed due to magnetic buoyancy, one would expect the strength of the toroidal field at the bottom of the convection zone to be depleted due to the action of magnetic buoyancy. One unphysical aspect of the non-local treatment of magnetic buoyancy is that this effect is usually not taken into account. As we have repeatedly pointed out, one require-

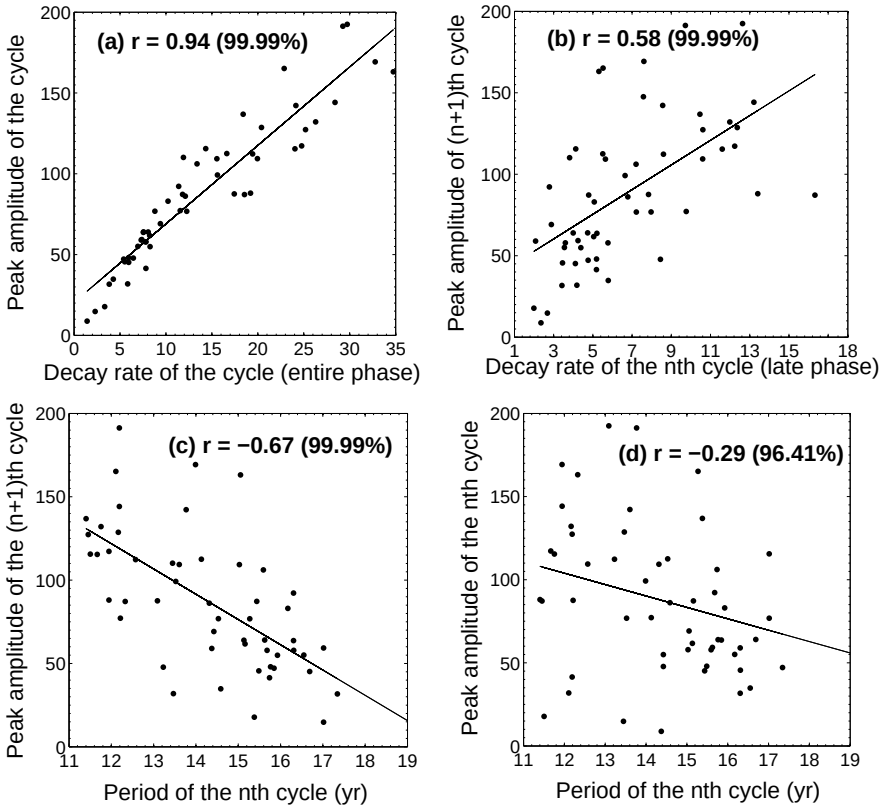
(a) r = 0.94 (99.99%)
Peak amplitude of the cycle
Decay rate of the cycle (entire phase)
(b) r = 0.58 (99.99%)
Peak amplitude of (n+1)th cycle
Decay rate of the nth cycle (late phase)
(c) r = −0.67 (99.99%)
Peak amplitude of the (n+1)th cycle
Period of the nth cycle (yr)
(d) r = −0.29 (96.41%)
Peak amplitude of the nth cycle
Period of the nth cycle (yr)

Figure 10. Same as Figure 8 but in this model, the large-scale flow has three cells radially stacked in the solar convection zone and the differential rotation includes near surface shear layer.

ment for obtaining the Waldmeier effect as well as the correlations discussed in this paper is that the effect of diffusivity has to be more important than the effect of toroidal field generation. Since the first method of treating magnetic buoyancy (used in the earlier subsections) puts a cap on the strength of the toroidal field but not the second non-local method, toroidal field generation remains unrealistically strong in the second method and it is more difficult to get the correlations properly in this method. We have taken the magnetic energy density (B^2) at latitude 15° at the bottom of the convection zone as the proxy of the sunspot number. In the first method of treating magnetic buoyancy (with the single-cell meridional circulation, as presented in Section 4.1–3), we found that all the correlations come out robustly if we use the magnetic energy density (B^2) in a wide range of latitudes as a proxy of the sunspot number. However, on using the second method of non-local magnetic buoyancy, we find that the magnetic energy density (B^2) has to be taken in a narrow band of low latitudes, with the correlations disappearing or even reversing if we use the magnetic energy density at higher latitudes. To sum up, the second non-local method of treating

magnetic buoyancy is a more robust method and keeps the dynamo stable over a wide range of parameters (which is not the case with the first method). However, it is more difficult to reproduce various observed correlations of the solar cycle with this non-local buoyancy method because the depletion of magnetic field due to buoyancy is not included.

5. Conclusion

We have discussed three important features of solar cycle – i) a linear correlation between the amplitude of cycle and its decay rate, ii) a linear correlation between the amplitude of cycle n and the decay rate of cycle $n-1$ and iii) an anti-correlation between the amplitude of cycle n and the period of cycle $n-1$. We have seen that all these correlations exist in all the data sets considered here. Last two correlations involve characteristics of one cycle and the amplitude of the next. So they provide useful precursors for predicting a future cycle. Just by measuring the period and the decay rate of a cycle, we can get an idea of the strength of the next cycle.

We have also explored whether these features can be explained in a B-L type flux transport dynamo model. We have first introduced stochastic fluctuations in the poloidal field generation (B-L α term) and we find that only the correlation between the decay rate and the cycle amplitude is reproduced. However when we added fluctuations in the meridional circulation, we found that all three correlations are reproduced in qualitative agreement with observational data. In our high diffusivity dynamo model, strong meridional circulation makes the period shorter and the decay rate faster, but it also makes the next cycle stronger—especially because the cycle strength displays a memory effect, depending on the meridional circulation a few years earlier. The opposite case happens when meridional circulation becomes weaker. Therefore the fluctuations in the meridional circulation are essential to reproduce the observed features. This study is consistent with earlier studies for modeling the cycle durations and strengths of observed cycles (Karak, 2010), the Waldmeier effect (Karak and Choudhuri, 2011), grand minima (Choudhuri and Karak, 2012) and few others (Passos, 2012) which indicate that the variable meridional circulation is crucial in modeling many aspects of the solar cycle. We have found that the observed correlations are reproduced even when the meridional circulation is assumed to be more complicated than the one-cell pattern used in most flux transport dynamo models. However, the coherence time of the fluctuations in the meridional circulation has to be not less than the cycle period in order to produce the correlations. The correlations disappear on making the coherence time too short, implying that fluctuations in the meridional circulation having coherence time of the order of convective turnover time cannot be the cause of the observed correlations. The theory of meridional circulation is still very poorly understood and we have no understanding of what may cause the fluctuations in meridional circulation with long coherence time. However, the pattern in the periods of the past cycles indicate the presence of such fluctuations (Karak and Choudhuri 2011) and the fact that only such fluctuations can explain the various

observed correlations of the solar cycle convinces us that such fluctuations in the meridional circulation with long coherence time must exist.

We have pointed out that the period or the decay rate of a cycle may be used to predict the next cycle, since these quantities indicate the strength of the meridional circulation which also determines the amplitude of the next cycle a few years later (due to the memory effect). It seems that the decay rate during the late phase of the cycle is the most reliable precursor for the next cycle, as seen in Figure 2(b)—presumably because the decay rate during this phase is the best indicator of the meridional circulation during the particular interval of time which is most crucial in determining the amplitude of the next cycle. However, fluctuations in the poloidal field generation process degrades all the observed correlations. As a result, even Figure 2(b)—displaying the correlation between the decay rate during the late phase and the amplitude of the next cycle—has considerable scatter, limiting our ability to predict the next cycle in this way.

Acknowledgment

This work is partly supported by DST through the J. C. Bose Fellowship awarded to ARC. GH thanks CSIR, India for financial support. We thank an anonymous referee for careful reading and providing constructive comments that helped to improve the quality of the paper.

References

Babcock, H.W.: 1961, *Astrophys. J.* **133**, 572. DOI. ADS.
Belvedere, G., Kuzanyan, K.M., Sokoloff, D.: 2000, *Mon. Not. Roy. Astron. Soc.* **315**, 778. DOI. ADS.
Brown, G.M.: 1976, *Mon. Not. Roy. Astron. Soc.* **174**, 185. ADS.
Cameron, R., Schüssler, M.: 2007, *Astrophys. J.* **659**, 801. DOI. ADS.
Cameron, R., Schüssler, M.: 2008, *Astrophys. J.* **685**, 1291. DOI. ADS.
Cameron, R.H., Dasi-Espuig, M., Jiang, J., Işık, E., Schmitt, D., Schüssler, M.: 2013, *Astron. Astrophys.* **557**, A141. DOI. ADS.
Charbonneau, P.: 2010, *Living Rev. Solar Phys.* **7**, 3. DOI. ADS.
Charbonneau, P., Dikpati, M.: 2000, *Astrophys. J.* **543**, 1027. DOI. ADS.
Chatterjee, P., Nandy, D., Choudhuri, A.R.: 2004, *Astron. Astrophys.* **427**, 1019. DOI. ADS.
Chou, D.-Y., Dai, D.-C.: 2001, *Astrophys. J. Lett.* **559**, L175. DOI. ADS.
Choudhuri, A.R.: 1992, *Astron. Astrophys.* **253**, 277. ADS.
Choudhuri, A.R.: 2011, *Pramana* **77**, 77. DOI. ADS.
Choudhuri, A.R., Karak, B.B.: 2009, *Res. Astron. Astrophys.* **9**, 953. DOI. ADS.
Choudhuri, A.R., Karak, B.B.: 2012, *Phys. Rev. Lett.* **109**, 171103. DOI. ADS.
Choudhuri, A.R., Chatterjee, P., Jiang, J.: 2007, *Phys. Rev. Lett.* **98**, 131103. DOI. ADS.
Choudhuri, A.R., Nandy, D., Chatterjee, P.: 2005, *Astron. Astrophys.* **437**, 703. DOI. ADS.
Choudhuri, A.R., Schussler, M., Dikpati, M.: 1995, *Astron. Astrophys.* **303**, L29. ADS.
Dasi-Espuig, M., Solanki, S.K., Krivova, N.A., Cameron, R., Peñuela, T.: 2010, *Astron. Astrophys.* **518**, A7. DOI. ADS.
Dikpati, M., Corbard, T., Thompson, M.J., Gilman, P.A.: 2002, *Astrophys. J. Lett.* **575**, L41. DOI. ADS.
D'Silva, S., Choudhuri, A.R.: 1993, *Astron. Astrophys.* **272**, 621. ADS.
Durney, B.R.: 1995, *Solar Phys.* **160**, 213. DOI. ADS.
Goel, A., Choudhuri, A.R.: 2009, *Res. Astron. Astrophys* **9**, 115. DOI. ADS.
Guerrero, G., de Gouveia Dal Pino, E.M.: 2008, *Astron. Astrophys.* **485**, 267. DOI. ADS.
Guerrero, G.A., Muñoz, J.D.: 2004, *Mon. Not. Roy. Astron. Soc.* **350**, 317. DOI. ADS.

Hathaway, D.H., Rightmire, L.: 2010, *Science* **327**. DOI. ADS.
Hathaway, D.H., Wilson, R.M., Reichmann, E.J.: 2002, *Solar Phys.* **211**, 357. DOI. ADS.
Hazra, G., Karak, B.B., Choudhuri, A.R.: 2014, *Astrophys. J.* **782**, 93. DOI. ADS.
Hotta, H., Yokoyama, T.: 2010, *Astrophys. J. Lett.* **714**, L308. DOI. ADS.
Jiang, J., Cameron, R.H., Schüssler, M.: 2014, *Astrophys. J.* **791**, 5. DOI. ADS.
Jiang, J., Chatterjee, P., Choudhuri, A.R.: 2007, *Mon. Not. Roy. Astron. Soc.* **381**, 1527. DOI. ADS.
Kane, R.P.: 2008, *J. Atmos. Solar-Terr. Phys.* **70**, 1533. DOI. ADS.
Karak, B.B.: 2010, *Astrophys. J.* **724**, 1021. DOI. ADS.
Karak, B.B., Choudhuri, A.R.: 2011, *Mon. Not. Roy. Astron. Soc.* **410**, 1503. DOI. ADS.
Karak, B.B., Choudhuri, A.R.: 2013, *Res. Astron. Astrophys.* **13**, 1339. DOI. ADS.
Karak, B.B., Nandy, D.: 2012, *Astrophys. J. Lett.* **761**, L13. DOI. ADS.
Karak, B.B., Kitchatinov, L.L., Choudhuri, A.R.: 2014, *Astrophys. J.* **791**, 59. DOI. ADS.
Karak, B.B., Jiang, J., Miesch, M.S., Charbonneau, P., Choudhuri, A.R.: 2014a, *Space Sci. Rev.* **186**, 561. DOI. ADS.
Karak, B.B., Rheinhardt, M., Brandenburg, A., Käpylä, P.J., Käpylä, M.J.: 2014b, *Astrophys. J.* **795**, 16. DOI. ADS.
Karak, B.B., Käpylä, P.J., Käpylä, M.J., Brandenburg, A., Olspert, N., Pelt, J.: 2015, *Astron. Astrophys.* **576**, A26. DOI. ADS.
Kitchatinov, L.L., Olemskoy, S.V.: 2011, *Astron. Lett.* **37**, 656. DOI. ADS.
Küker, M., Rüdiger, G., Schultz, M.: 2001, *Astron. Astrophys.* **374**, 301. DOI. ADS.
Lantos, P.: 2000, *Solar Phys.* **196**, 221. DOI. ADS.
Leighton, R.B.: 1969, *Astrophys. J.* **156**, 1. DOI. ADS.
Longcope, D., Choudhuri, A.R.: 2002, *Solar Phys.* **205**, 63. DOI. ADS.
Lopes, I., Passos, D.: 2009, *Mon. Not. Roy. Astron. Soc.* **397**, 320. DOI. ADS.
Muñoz-Jaramillo, A., Dasi-Espuig, M., Balmaceda, L.A., DeLuca, E.E.: 2013, *Astrophys. J. Lett.* **767**, L25. DOI. ADS.
Nandy, D., Choudhuri, A.R.: 2002, *Science* **296**, 1671. DOI. ADS.
Ogurtsov, M., Lindholm, M.: 2011, *ISRN Astron. Astrophys.* **2011**, 3. DOI. ADS.
Parker, E.N.: 1955a, *Astrophys. J.* **122**, 293. DOI. ADS.
Parker, E.N.: 1955b, *Astrophys. J.* **121**, 491. DOI. ADS.
Passos, D.: 2012, *Astrophys. J.* **744**, 172. DOI. ADS.
Passos, D., Lopes, I.: 2012, *Mon. Not. Roy. Astron. Soc.* **422**, 1709. DOI. ADS.
Passos, D., Charbonneau, P., Beaudoin, P.: 2012, *Solar Phys.* **279**, 1. DOI. ADS.
Priyal, M., Banerjee, D., Karak, B.B., Muñoz-Jaramillo, A., Ravindra, B., Choudhuri, A.R., Singh, J.: 2014, *Astrophys. J. Lett.* **793**, L4. DOI. ADS.
Schad, A., Timmer, J., Roth, M.: 2013, *Astrophys. J. Lett.* **778**, L38. DOI. ADS.
Solanki, S.K., Krivova, N.A., Schüssler, M., Fligge, M.: 2002, *Astron. Astrophys.* **396**, 1029. DOI. ADS.
Svalgaard, L., Cliver, E.W., Kamide, Y.: 2005, *Geophys. Res. Lett.* **32**, 1104. DOI. ADS.
Wang, Y.-M., Sheeley, N.R. Jr.: 1989, *Solar Phys.* **124**, 81. DOI. ADS.
Wang, Y.-M., Sheeley, N.R. Jr., Nash, A.G.: 1991, *Astrophys. J.* **383**, 431. DOI. ADS.
Watari, S.: 2008, *Space Weather* **6**, 12003. DOI. ADS.
Yeates, A.R., Nandy, D., Mackay, D.H.: 2008, *Astrophys. J.* **673**, 544. DOI. ADS.
Yoshida, A., Yamagishi, H.: 2010, *Ann. Geophysicae* **28**, 417. DOI. ADS.
Zhao, J., Bogart, R.S., Kosovichev, A.G., Duvall, T.L. Jr., Hartlep, T.: 2013, *Astrophys. J. Lett.* **774**, L29. DOI. ADS.